Available online at www.sciencedirect.com
SCIENCE DIRECT®
Coordination Chemistry Reviews 249 (2005) 1518–1535
COORDINATION CHEMISTRY REVIEWS
www.elsevier.com/locate/ccr

Review

Some general principles for designing electrocatalysts with hydrogenase activity

Vincent Artero*, Marc Fontecave

Laboratoire de Chimie et Biochimie des Centres Rédox Biologiques, UMR 5047 CEA/CNRS/Université Joseph Fourier, CEA-Grenoble, DRDC/CB, 17 rue des Martyrs, 38054 Grenoble Cedex 09, France

Received 13 May 2004; accepted 23 January 2005
Available online 23 February 2005

Contents

Abbreviations: app., apparent; bipy, bipyridine; $^{bu}S_4^{2-}$, 1,2-bis(2-mercapto-3,5-di-*t*-butylphenylthio)ethane dianion; CB, conduction band; Cp^-, cyclopentadienyl anion; Cp^{*-}, pentamethylcyclopentadienyl anion; Cy, cyclohexyl; cyclam, 1,4,8,11-tetraazacyclotetradecane; dape, 1,2-bis{di(*p*-methoxyphenyl)phosphino}ethane; depp, 1,3-bis(diethylphosphino)propane; dmf, dimethylformamide; dmg^{2-}, dimethylglyoximato dianion; dmpm, bis(dimethylphosphino)methane; dmso, dimethylsulfoxide; DPB, diporphyrinatodiphenylene; dppe, 1,2-bis(diphenylphosphino)ethane; dppf, 1,1′-bis(diphenylphosphino)ferrocene; dppm, bis(diphenylphosphino)methane; dtfpe, 1,2-bis{bis(*p*-trifluoromethyl)phenyl phosphino}ethane; [Fe], iron; g^{2-}, glyoximato dianion; GC, gas chromatography; *L, 1-*t*-butyl-5-phenylimidazole; MS, mass spectrometry; MV, methylviologen; [NiFe], nickel–iron; OEP, octaethylporphyrin; Pc, phtalocyanine; $py^{bu}S_4^{2-}$, 2,6-bis(2-sulfanyl-3,5-di-*t*-butylphenylthio)dimethylpyridine dianion; SHE, standard hydrogen electrode; S_3^{2-}, bis(2-sulfanylphenyl)sulfide dianion; TOF, turnover frequency; TON, turnover number; TPP, tetraphenylporphyrin; THF, tetrahydrofuran

* Corresponding author. Tel.: +33 4 38 78 91 06; fax: +33 4 38 78 91 24.
E-mail address: vartero@cea.fr (V. Artero).

doi:10.1016/j.ccr.2005.01.014

Abstract

Hydrogenases are enzymes that catalyze the reversible interconversion between hydrogen and protons with remarkable efficiency. On the other hand, the design of synthetic electrocatalysts for proton reduction or hydrogen oxidation has been a goal sought for decades, even before the crystallographic determinations of the structure of hydrogenases, namely because of the important technological applications of these reactions (H_2 production and fuel cells). This paper reviews the pre-biomimetic functional systems with regard to their mechanism, activity (depending on the assays) and performances (cost, efficiency, robustness). We show how the design of new bio-inspired catalysts should integrate the structural characteristics found at the active sites, in particular those specifically relevant to the activity, but also benefit from the former studies on non-biomimetic systems.

Keywords: Hydrogenase; Catalysis; Proton reduction; Hydrogen oxidation; Biomimetic modelization; Bioinorganic chemistry

1. Introduction

Molecular hydrogen is expected to be the major energy carrier in global human activity in the XXIth century. However, because of intrinsic kinetic limitations, only high temperature or platinum-catalyzed devices are currently economically viable for the production or the uptake of molecular hydrogen [1]. For this reason, the design of effective catalysts for proton reduction or hydrogen oxidation has become a challenge for the chemical community. To date, no molecular system but hydrogenases can achieve this goal. These enzymes [2] are divided into two classes depending on the metal content at the active site: [Fe]-only and [NiFe] hydrogenases.[1] The structures of both classes have been recently published [3]. Both are electrochemically characterized by a quasi-nerstian behavior [4], making the enzymes themselves or chemical biomimetic models [5] very attractive for biotechnological applications during the last 5 years.

However, despite significant achievements in the structural modelization of [Fe]-only hydrogenases [6], the new biomimics show little activity associated with high overvoltages so that immediate optimization perspectives appear quite limited.

A first level of modelization results in structural biomimetics. Based on structural information of the enzyme metal centers, the synthetic analogue strategy, as defined by Ibers and Holm [7], indeed allows us to define the minimal structure required for a catalyst to achieve the biological function. However, a purely structural approach may not be the most adequate one for the elaboration of highly active catalysts, since the biomolecular environment (active site) actually plays a key role and should also be modelized. A first solution is the introduction of minor structural and electronic modifications into the biomimetic compound, provided that the basic structure–function relationships of the enzyme center are conserved [8]. However, it could be worth taking the problem from another angle, starting from an active or potentially active non-biomimetic system (different ligands, different metals) and introducing new structural or electronic properties inspired from the structure of the active sites of the enzymes. These should not be called bio-mimetic but bio-inspired models instead.

Since the publication of the crystallographic structures of hydrogenases, studies concerning non-biomimetic but active or potentially active systems seem to have been abandoned. Transition metal catalyzed proton reduction was first reviewed by Kölle in 1992 [9]. In this paper, we provide a review of the most efficient catalysts for hydrogen production/uptake highlighting the different structural and electronic features in relation with their activity but also their limitations in terms of technological applications. We will try to define the general principles for the design of new, bio-inspired, economically viable catalysts for proton reduction or hydrogen oxidation.

2. Hydrogen production/uptake by the hydrogenase enzymes

The structures of the active site of both kinds of hydrogenases, as revealed by single crystal X-ray determinations, are given in Fig. 1 [3].

[Fe]-only hydrogenases are 50–100 times more active than [NiFe] hydrogenases. Typical activities for [Fe]-only

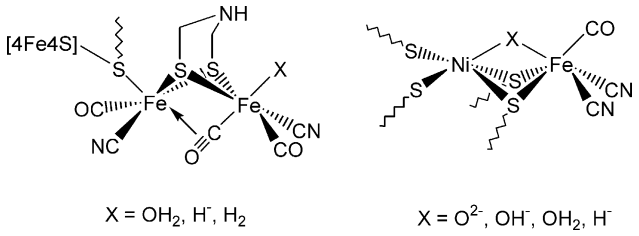

Fig. 1. Structures of the active sites of [Fe]-only (left) and [NiFe] (right) hydrogenases (X are putative ligands).

[1] A third class of hydrogenases, hitherto called "metal-free hydrogenases" is described. A recent report from Thauer [E.J. Lyon, S. Shima, G. Buurman, S. Chowdhuri, A. Batschauer, K. Steinbach, R.K. Thauer, Eur. J. Biochem. 271 (2004) 195; S. Shima, E.J. Lyon, M. Sordel-Klippert, M. Kauss, J. Kahnt, R.K. Thauer, K. Steinbach, X. Xie, L. Verdier, C. Griesinger, Angew. Chem. Int. Ed. 43 (2004) 2547] reveals that these enzymes contain an iron cofactor and should be called "iron–sulfur cluster free hydrogenases" instead. These enzymes however do not catalyze the $\{H_2/2H^+ + 2e^-\}$ interconversion but the hydride transfer from H_2 to methenyltetrahydromethanopterin.

hydrogenases are 5–10 mmol H_2 min^{-1} mg^{-1} protein for hydrogen evolution and 10–50 mmol H_2 min^{-1} mg^{-1} protein for hydrogen uptake with K_M values for H_2 in the range 0.1–1 mM at 30 °C and pH 8. This corresponds to maximum turnover frequencies in the range 6000–60,000 molecules H_2 s^{-1} per site; [NiFe] hydrogenases have in contrast two order of magnitude lower K_M values but also lower activities, in both hydrogen evolution and uptake (0.1–1 mmol H_2 min^{-1} mg^{-1} protein, i.e. 100–1000 molecule H_2 s^{-1} per site) [10]. Nevertheless, these values strongly depend on the type of activity assay. The quite low activities of [NiFe] H_2ases measured using redox dyes are possibly due to the limitation of the reaction rate by the electron transfer step between the reduced dye and the enzyme [11]. Accordingly, electrochemical experiments with the [NiFe] hydrogenase of *Chromatium vinosum* recently led to higher activity values such as 1500–9000 molecule H_2 s^{-1} per site for hydrogen consumption depending on the electroactive coverage of the electrode. Moreover, a graphite electrode coated with a [NiFe] hydrogenase has the same reversible behavior as a platinum electrode [4], so that, under these conditions, a single enzymatic site is two orders of magnitude more active than a platinum atom on the metallic surface [12].

Both classes of hydrogenases are able to catalyze either proton reduction or hydrogen oxidation but it is commonly claimed, according to their different affinities for molecular hydrogen, that [Fe]-only hydrogenases have greater activity for H_2 production, while [NiFe] hydrogenases are more efficient for hydrogen uptake. These two processes have very different pH optima but electrochemical measurements on adsorbed enzymes at carbon electrode over the entire pH range confirm these general trends for both [Fe]-only [13] and [NiFe] [11] hydrogenases. For example, the largest electrochemically measured reductive activity, at low pH, of the [NiFe] hydrogenase of *C. vinosum* is one order of magnitude smaller than its oxidative counterpart, which is not pH-dependent.

The activity in proton reduction is strongly inhibited upon exposure to oxidative conditions [14], not only when the enzyme is exposed to oxygen but also, in the case of *C. vinosum* [11,15] or *D. gigas* [16] [NiFe] hydrogenases, when the enzyme is held at potentials more positive than −160 to −100 mV/SHE. In the case of [NiFe] hydrogenases, this inactivation is a slow [17] and reversible process.

Furthermore, proton reduction is also inhibited by the presence of hydrogen in solution [11], and given the low K_M values for H_2 in the case of [NiFe] hydrogenases, this can explain the low activity of this class of enzymes for proton reduction.

The heterolytic nature of hydrogen cleavage by hydrogenase was first established by Krashna, studying the isomerization of *para*-hydrogen into *ortho*-hydrogen in the presence and in the absence of hydrogenases [10,18]. Hydrogen/deuterium exchange [19] using H_2 and D_2O (Eq. (1)) or D_2 and H_2O (Eq. (2)) and measuring the formation rate of HD gas is currently widely used as an assay [20].

$$H_2 + D_2O \rightleftharpoons HD + HDO \quad (1)$$

$$D_2 + H_2O \rightleftharpoons HD + HDO \quad (2)$$

3. Mechanistic features of hydrogen production/uptake

The terms “hydrogen production” or “uptake” have different interpretations since they just determine the final product or the starting material of the reaction. In this paper, we will focus on the hydrogenase activity, which exclusively concerns the interconversion between H_2 and $2e^- + 2H^+$, the electrons being kept at a potential close to the apparent standard potential of the H^+/H_2 couple in the solution. Note that such reactions thus have a very low driving force. It is significantly more difficult to achieve than the reduction of substrates such as $NAD(P)^+$ by H_2 via hydride transfer or hydrogenation reaction, during which a significant part of the reducing power is converted into heat during the reaction. Such reactions will be excluded from this account.

The $\{H_2/2H^+ + 2e^-\}$ interconversion is a two-electron process and the related reactions should involve either a $H^\bullet$ radical or a hydride ion. The very low potentials of the $H^+/H^\bullet$ ($E^\circ = -2.29$ V/SHE in water) and H^+/H^- ($E^\circ = -1.05$ V/SHE in water) couples [21] preclude the involvement of free $H^\bullet$ or H^- as intermediates. Indeed, because of the reversible adsorption of H_2 and stabilization of adsorbed $H^\bullet$ on platinum, palladium and nickel surfaces, the reduction of protons and the oxidation of hydrogen occur with low overvoltages through a “homolytical” mechanism. In contrast, these reactions always proceed in solution via a “heterolytic” pathway involving a hydride ion stabilized through some chemical interaction with the catalysts (Fig. 2).

As far as homogeneous catalysis is concerned, the mechanism of hydrogen production/uptake always implies, in one of the intermediate or activated states, the coordination of molecular hydrogen, the formation of hydride species and the transfer of two electrons. Coordination complexes are thus naturally suited for such a catalysis since they combine both redox and acid–base reactivities.

The general mechanistic schemes are given in Fig. 3. Clockwise rotation through the cycle corresponds to proton reduction, whereas counterclockwise rotation involves hydrogen oxidation. The pathways are then quite different depending on whether the formation or the cleavage

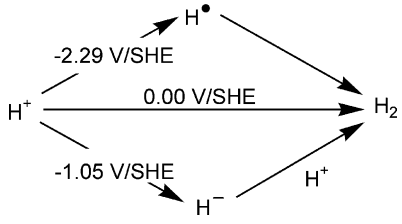

Fig. 2. Proton reduction to dihydrogen [21].

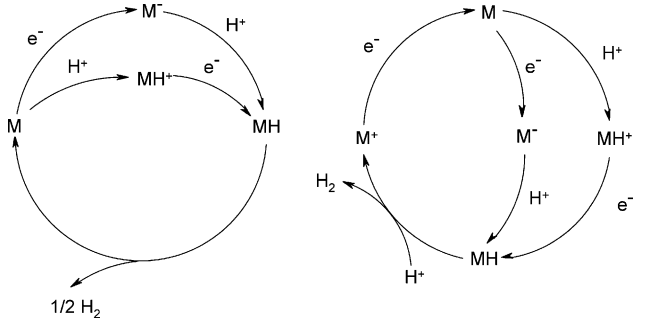

Fig. 3. Homolytic (left) and heterolytic (right) pathways for proton reduction catalyzed by a coordination compound.

of the H–H bond occurs via a homolytic or heterolytic pathway.

In the homolytic mechanism, two metallic catalytic centers are usually required. Regarding proton reduction, two key steps can be identified: In the first one, both metal centers are protonated to give metal hydride complexes. H_2 evolution subsequently results from a reductive elimination reaction from these two metal hydride moieties. The third step, a monoelectronic reduction can occur either at the unprotonated metal state or once the hydride species formed.

H_2 oxidation proceeds via coordination at one metal center or, as a bridge, between two metal centers, followed by a bimetallic oxidative addition reaction yielding two metal hydride moieties. For both reactions, the metals then stock one redox equivalent each and switch between two redox states, thus avoiding any disproportionation reactions. Espenson et al. and Spiro et al. developed cobaloximes [22] and cobalt porphyrins [23], respectively, that evolve hydrogen through such a mechanism. Collman et al. also demonstrated that the ruthenium porphyrin [Ru(OEP)(thf)] (**1**) catalytically oxidize hydrogen with a 150 mV overpotential at pH 13 [24]. The active species is a cofacial bisporphyrin complex $[Ru(OEP)]_2$ ($\mathbf{1}'_2$) which is first electrochemically reduced to the "dimer dianion" $[Ru(OEP)]_2^{2-}$ form, then able to oxidatively add hydrogen across its single metal-metal bond to give two ruthenium(II) hydrides. The latter are subsequently oxidized and deprotonated to restore the catalyst as the "dimer dianion" form (Fig. 4).

This process is however not kinetically favorable since the rate of a step which is second order with regard to the catalyst is necessarily slow. Furthermore, this precludes any further controlled immobilization of the catalyst on a surface of an electrode since two different immobilized centers will not be able to react together. Nevertheless, these drawbacks can be overcome by the design of bimetallic catalysts (Fig. 5). Collman et al. developed such a strategy for a series of cofacial metallodiporphyrins [25], such as $[Ru_2(DPB)]$ (**2**) without any significant improvement of the catalytic features by comparison with other monometallic porphyrin complexes. This approach was more successful using the bridged bismetallocene **3** and **4** in which two metal centers are held close together, as developed by Bitterwolf et al. [26] and Mueller-Westerhoff et al. [27]. [1.1]Ferrocenophane (**3**) shows high activity in photoelectrochemical production of hydrogen (see below). Lastly, a reaction mechanism involving a dihydride intermediate might account for the higher activity of the binuclear $[Ni_2(biscyclam)]^{4+}$ ($\mathbf{5}^{4+}$) over the mononuclear $[Ni(cyclam)]^{2+}$ ($\mathbf{6}^{2+}$) [28].

An alternative, heterolytic, pathway (Fig. 3) was proposed in which the resulting metal hydride decomposes by proton attack, rather than by disproportionation of two metal hydride, to evolve hydrogen, probably via an intermediate dihydrogen metal complex. Such a mechanism was ascertained using cyclovoltametry by Savéant and co-workers for proton reduction electrocatalyzed by iron (**7Cl**) (Fig. 6) [29] and rhodium (**8Cl**) (Fig. 18) [30] porphyrins complexes. The reverse mechanism (Fig. 7) was proposed for hydrogen oxidation catalyzed by the complex $[Ni\{(Et_2PCH_2)_2NMe\}_2]^{2+}$ ($\mathbf{9}^{2+}$) prepared by DuBois and co-workers [31].

In contrast with the former mechanism, no step in this scheme is second order with regard to catalyst concentration, which could result in a kinetic bottleneck. As another striking difference with the homolytic mechanism, the metal center now shuttles between three distinct oxidation states, which expands the catalytic cycle over a wider range of electrochemical potentials. Moreover, disproportionation reactions between complexes in different redox states should be considered. The latter may be avoided, and the overall mechanism changed, upon grafting the catalyst on an electrode, since the active species will be held apart.

In some cases, proton reduction was shown to proceed by parallel heterolytic and homolytic mechanisms. This was established for example for the reaction of the hydridocobaloxime $[HCo(dmgH)_2(PBu_3)]$ (**10a**) with perchloric acid in methanol–water mixture [22]. In a first approach to discriminate between these mechanisms, Spiro, studying cobalt porphyrin electrocatalysts, examined the reaction schemes detailed below, both resulting in the net balance (5).

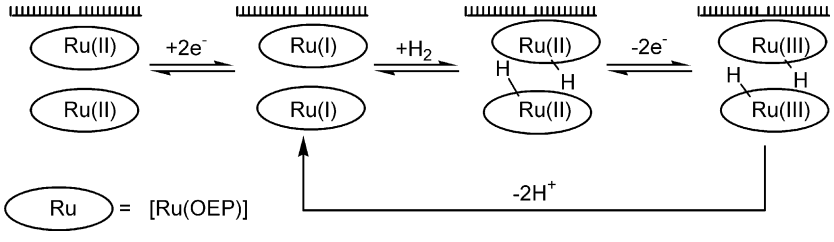

Fig. 4. Proposed mechanism for the hydrogen oxidation catalyzed by $[Ru(OEP)]_2$ ($\mathbf{1}'_2$) at a graphite electrode.

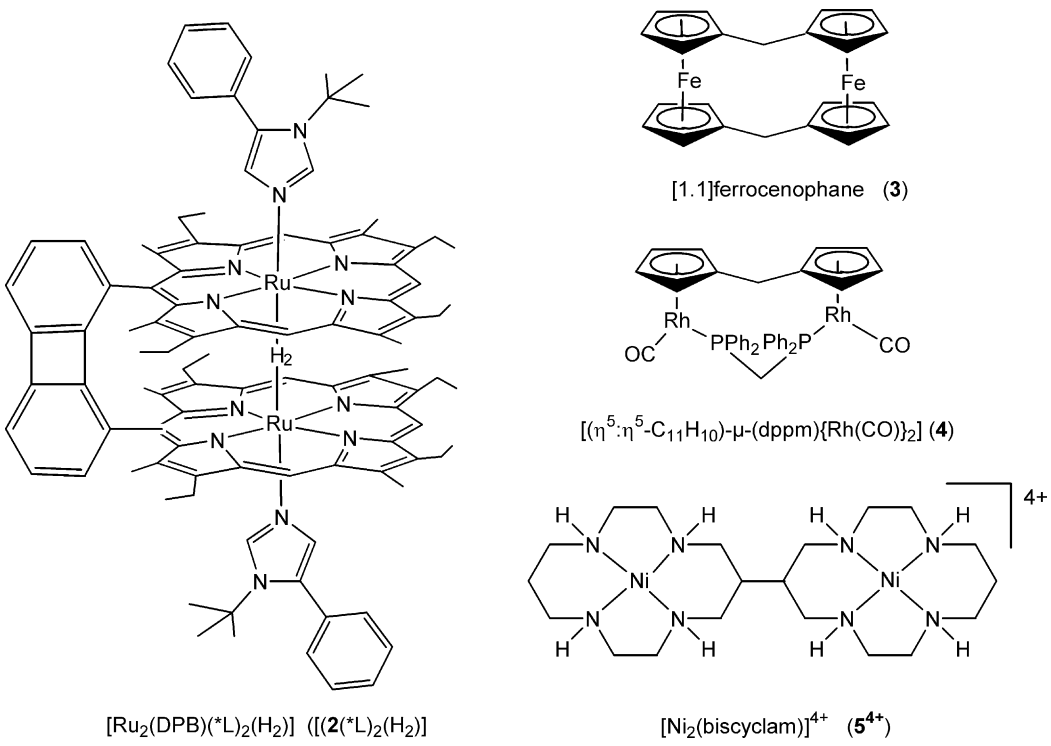

Fig. 5. Molecular structures of some binuclear catalysts for proton reduction and hydrogen oxidation.

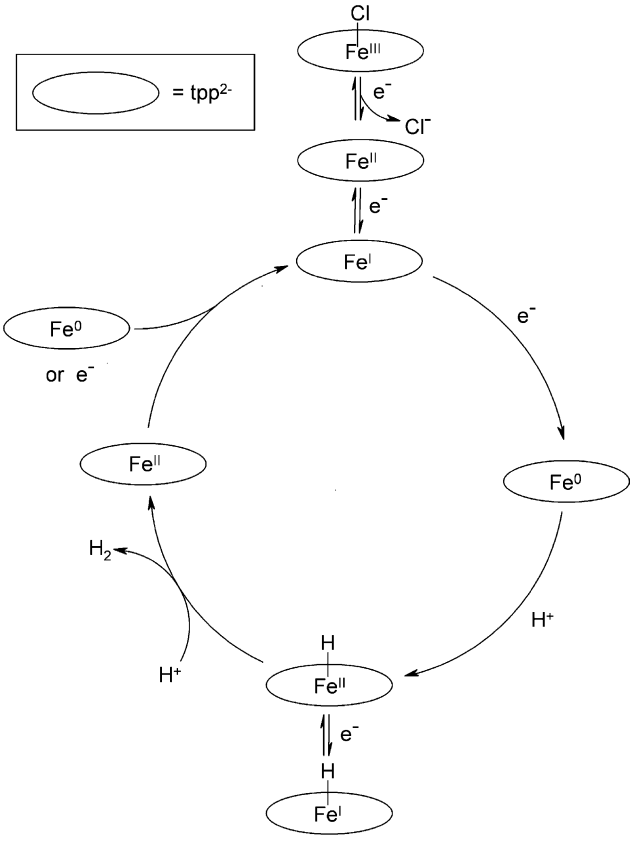

Fig. 6. Mechanism for the reduction of Et_3NH^+ to hydrogen catalyzed by [Fe(TPP)Cl] (**7Cl**) in DMF (global charges of the complexes are not indicated).

Given the electrochemical characteristics of the catalyst and the operating conditions (pH, $P(H_2)$, temperature, solvent ...), this led to the determination of the electromotive forces of reactions (3) (homolytic pathway) and (4) (heterolytic pathway) and allowed identifying the most thermodynamically favored process [23].

$$\tfrac{1}{2}Co^{I} + H^{+} \rightleftharpoons \tfrac{1}{2}Co^{III} + \tfrac{1}{2}H_2 \quad (3)$$

$$\tfrac{1}{2}Co^{III} + \tfrac{1}{2}e^{-} \rightleftharpoons \tfrac{1}{2}Co^{II}$$

$$\tfrac{1}{2}Co^{II} + \tfrac{1}{2}e^{-} \rightleftharpoons \tfrac{1}{2}Co^{I}$$

$$E(3) = E(H^{+}/H_2) - \tfrac{1}{2}E(Co^{III}/Co^{II}) - \tfrac{1}{2}E(Co^{II}/Co^{I})$$

$$Co^{I} + H^{+} \rightleftharpoons Co^{II} + \tfrac{1}{2}H_2 \quad (4)$$

$$Co^{II} + e^{-} \rightleftharpoons Co^{I}$$

$$E(4) = E(H^{+}/H_2) - E(Co^{II}/Co^{I})$$

$$H^{+} + e^{-} \rightleftharpoons \tfrac{1}{2}H_2 \quad (5)$$

4. The evaluation of functional models

Catalysts for proton reduction or hydrogen oxidation are essentially characterized by their turnover frequency, their working overpotential and their robustness (total turnover

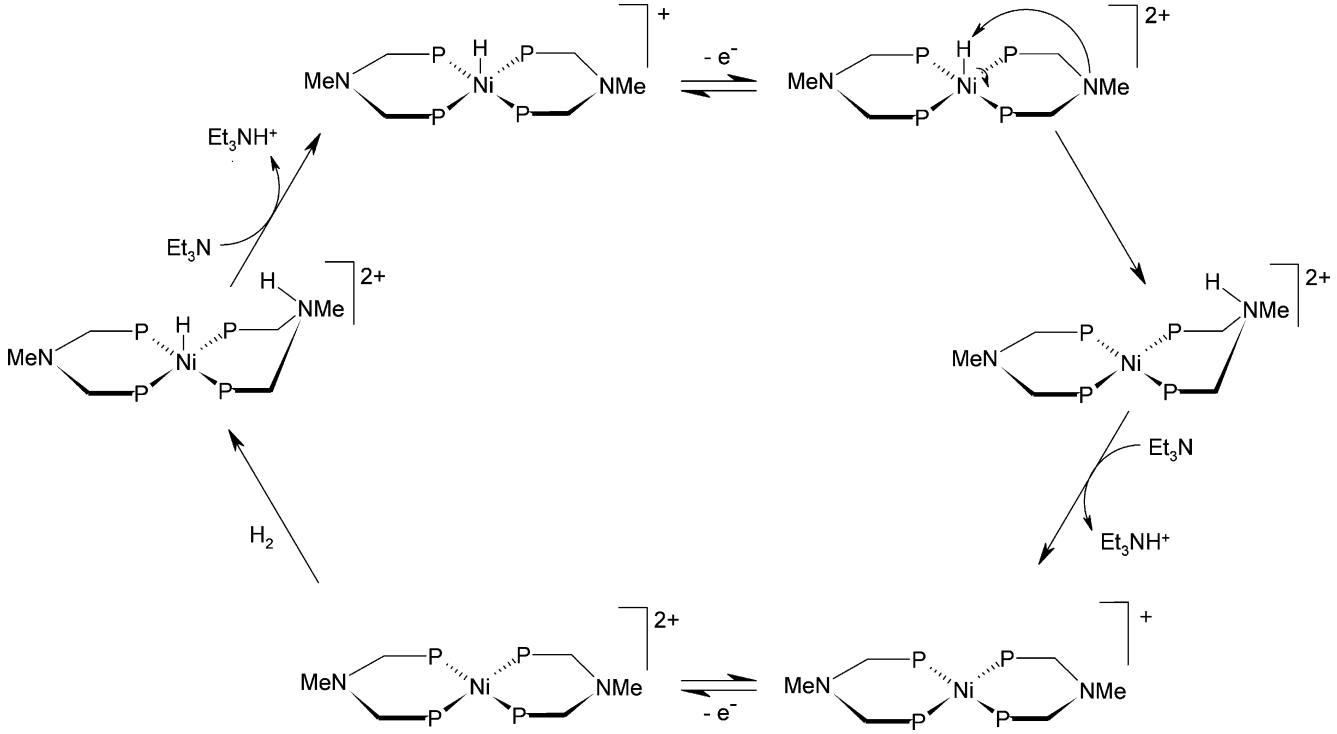

Fig. 7. Proposed mechanism for the oxidation of hydrogen catalyzed by $[Ni\{(Et_2PCH_2)_2NMe\}_2]^{2+}$ ($\mathbf{9}^{2+}$) in CH_3CN.

number). It could be useful to properly define this notion of overpotential, which is specific to electrochemical applications. Indeed, the potential at which electrocatalysis takes place is not relevant for the evaluation of the catalyst, but the overpotential is. It is defined as the difference between the potential at which catalysis is achieved and the apparent thermodynamic potential of the H^+/H_2 couple under the operating conditions. Note that, for thermodynamic reasons, the measured potential is always more negative (respectively positive) than, or equal to, the apparent potential of the H^+/H_2 couple for proton reduction (respectively hydrogen oxidation). Overpotential may be caused by slow kinetics of charge transfer, mass transport and/or ionic transport. The overpotential arising from slow kinetics of charge transfer, the one that electrocatalysis can overcome, is usually termed as the activation overpotential.

When a given synthetic complex catalyzes proton reduction with overpotential, the same complex is not thermodynamically competent for catalyzing H_2 oxidation using the microscopic reverse of the former reaction. This is in marked contrast with hydrogenases, which, because they do not display any overpotential, are able to catalyze both processes. Electrocatalytic reduction of protons and hydride transfer reactions were reviewed recently by Deronzier and Moutet [32].

4.1. Activity assays

Electrocatalytic reactions differ from bulk catalytic applications since they are evaluated in terms of both Faradaic (selectivity, conversion) and energetic yield, defined as the balance between the mobilized electric energy and the recovered chemical energy and mainly characterized by the overpotential observed for the process. Electrochemistry is the method of choice for the evaluation of electrocatalysts since it allows the simultaneous determination of both thermodynamic and kinetic characteristics of the process: the rate of the catalyzed reaction is directly measured as a current upon varying the potential of the electrode. Catalytic waves can first be observed using cyclic voltammetry whereas electrolysis experiments, coupled to GC analysis of the evolved gas or analysis of the bulk composition, are further used to determine both the Faradaic yield and the stability (turnover number) of the catalyst.

Simulations of the cyclovoltamograms give some insight into the mechanism and allow an estimation of the kinetic and thermodynamic constants [29,30]. Cyclic voltammetry is unfortunately restricted to the characterization of fairly active species, i.e. with a second order rate constant of more than approximately 100 mol L^{-1} s^{-1} as estimated by DuBois and co-workers [31], but reveals all catalytic activities, even those associated with high overpotentials. For less active species, it is necessary to develop more sensitive kinetic tests. Biochemical activity assays for hydrogenases are usually based on the utilization of redox dyes, such as methylene blue ($E^{\circ app}$ = 0.01–0.03pH V/SHE), methylviologen (E° = −0.44 V/SHE) or benzylviologen (E° = −0.36 V/SHE) whose standard potentials [33] lay around the standard potential of the redox couple H^+/H_2 in aqueous pH 7 solutions: reduced dyes act as electron donors for proton reduction whereas oxidized one serve as electron acceptors in hydrogen

oxidation. Such an assay was adapted, albeit improperly (see below), by Hembre in non-aqueous solvents. The limitation of such assays is that they are restricted to systems catalyzing the $\{H_2/2H^+ + 2e^-\}$ interconversion with low overpotentials.

Another widely used activity test consists in measuring the rate of hydrogen/deuterium exchange catalysis between D_2 and H_2O or H_2 and D_2O. This can be done using GC/MS technique [34] or proton and deuterium NMR [35]. Such a reaction is specific for hydrogenase enzymes and their model compounds but does not provide any thermodynamic information since both reactions have zero standard free enthalpy variation. Completion of the catalytic cycle is even not ascertained since any complex able to activate hydrogen to form a metal hydride and a proton will be tested positive provided that this step is reversible. Moreover, applied pressures of H_2 and D_2, up to 35 bar are often used in order to obtain concentrations in dissolved H_2, HD or D_2 high enough to allow detection of the gases by NMR. Up to now, no correlation between the quantitative results obtained by electrochemical experiments and those arising from H/D exchange assays was reported.

4.2. Assays operating conditions

The optimization of the test relies on the clear choice of the solvent, pH (if applicable), potential and grafting conditions as discussed below.

4.2.1. Solvent

The active sites of hydrogenases are surrounded by hydrophobic peptidic residues. Moreover, their organometallic nature makes structural mimics more soluble in non-aqueous solvents than in water. This has led to the development of activity tests in acetone, propylene carbonate or acetonitrile for evaluation of model compounds. This is obviously not without consequences for the definition of pH and of the potential of the redox couples. The apparent potential of the reference couple, H^+/H_2, is indeed strongly dependent on the nature of the protic species (solvated protons or weak acid). Similarly, the electrochemical features and then the catalytic activity of the catalyst can be strongly influenced by the nature of the solvent. For example, the two-electron oxidation potential of $[Cp^*Rh^{I}L]$ (L = 2,2′-bipyridine-4,4′-dicarboxylic acid) (**11a**) varies from −0.65 V/SHE in acetonitrile to −0.53 V/SHE in alkaline pH 11 aqueous solution [36]. A similar 150 mV shift was observed for the electrochemical response of a similar $Cp^*Rh^{III}L$ complex electropolymerized at a carbon electrode when switching from acetonitrile to 0.1 mol L^{-1} $LiClO_4$, pH 5, aqueous solution [37].

4.2.2. Acidobasic conditions

The presence of an acid (respectively a base) strong enough to protonate (respectively deprotonate) the intermediate hydride in one of its redox states governs its reactivity in a key step of the catalytic cycle. In other words, chemical models, unlike enzymes, undergo general acid catalysis and both pH (acid/base concentration in non-aqueous solutions) and the pK_a of the acidobasic partner have to be considered. Indeed, whereas the iron(I) *meso*-tetraphenylporphyrin complex (**7**$^-$) displays electrocatalytic activity in DMF for the reduction of the weak Et_3NH^+ acid [29], the rhodium(I) porphyrin (**8**$^-$) indeed electrochemically catalyzes proton reduction in DMSO (Fig. 18) only if an acid stronger than formic acid is used [30].

Finally, the choice of the assay pH range also determines the working overpotential since the electrocatalytic wave usually developed from a given redox feature of the catalyst.

4.2.3. Potential

Special care should be taken when using a redox dye. The potential of reduction of methylviologen MV^{2+} to the cation–radical MV^+ is influenced by the presence of surfactants in the solution, which stabilizes the reduced species [38]. The same drastic effect is observed when switching to non-aqueous solvents. Cyclovoltamograms of $MV(PF_6)_2$ recorded in acetone or methanol show a first reversible monoelectronic transfer with cathodic and anodic peaks at −103 and −37 mV/SHE, respectively, far away from the −450 mV/SHE standard potential value that can be measured in physiological serum [38]. In the hydrogen oxidation assay developed by Hembre for the evaluation of $[Cp^*RuH(dppf)]$ (**12**) [39], the oxidized MV^{2+} is now strong enough to partially oxidize tetramethylpiperidine, first introduced as a Brönstedt base, in acetone at room temperature in the absence of the catalyst and hydrogen [40]. Thus, in this case, the reported reduction of MV^{2+} has been incorrectly assigned to hydrogen oxidation.

4.2.4. Grafting

The activity observed in homogeneous solution may not be reproducible with an active species anchored to an electrode. Spiro reported a series of cobalt porphyrins with high activity for H_2 production, associated with low overvoltage in neutral aqueous solution. However, these compounds proved difficult to handle when covalently grafted to an electrode via an amide link with surface carboxylic acid groups: film instability or disrupting processes at either film–electrode or film–electrolyte interfaces were postulated. Nevertheless, a stable catalyst system was obtained by incorporating positively charged cobalt porphyrin complexes into a Nafion membrane coated on a glassy carbon electrode but low electroactivity was observed, reflecting the poor electron-transfer characteristics of Nafion films [23]. Kanedo et al., however, reported good proton reduction activity around the equilibrium potential for neutral [Co(TPP)] (**13**) incorporated in a Nafion membrane coated on a platinum electrode in a pH 1 aqueous solution. In contrast, when coated on a bare pyrolytic graphite electrode, the same catalyst can reduce protons only with a larger overpotential (−0.7 V versus Ag/AgCl; pH 1) and a considerably lower 70 h^{-1} turnover frequency value [41]. Better catalytic activity such as 2×10^5 h^{-1} TOF was observed at a potential of −0.90 versus Ag/AgCl and

pH 1 for a cobalt phtalocyanine (**14**) incorporated in a poly(4-vinylpyridine-co-styrene) film coated on a graphite electrode. They also found that the catalytic proton reduction was limited by the electron transfer within the matrix [42]. Electropolymerization of $[Cp^*Rh(L)Cl](BF_4)$ (L = bis-(2-pyrrol-1-yl-1-pyrrol-1-yl methyl ethyl)-2,2′-bipyridinyl-4,4′-dicarboxylate) (**11b**(BF_4)) leads to a stable film capable of proton electroreduction at −0.31 V versus SHE at pH < 4. Quantitative current efficiency corresponding to 353 turnovers was observed during a 14 h electrolysis experiment at pH 1 using a carbon-felt electrode coated with the electropolymerized rhodium complex [37].

5. Specifications applicable to catalysts for proton reduction or hydrogen oxidation

The success of a catalyst is based on three characteristics: cost, efficiency and robustness.

5.1. A good catalyst is a cheap catalyst!

Hydrogenases are fascinating because they catalyze the fundamental $\{2H^+ + 2e^-/H_2\}$ interconversion at high rate and small overpotentials from equilibrium, using cheap first-row transition metals at the active sites. Modelization of these active clusters could lead to the replacement of unsustainable platinum electrocatalysts in electrolyzer/fuel cell applications. The replacement of platinum with inexpensive materials is critical to the large-scale utilization of hydrogen as a clean energy vector. This could however be less relevant as far as high-value added devices such as micro fuel cell for laptop or mobile phone are concerned.

5.2. A good catalyst is an economically viable catalyst!

Application of an electrocatalyst in large-scale electrolyzers or fuel cells obviously requires high turnover frequencies to achieve high currents and low overpotential. Up to now, no synthetic molecular catalyst would have the potential to compete with platinum or nickel based (Pt/C, PtMo/C, PtRu/C, Raney-Ni . . .) or other composite (C/W, NiFeZn, electrodeposited heteropolyanions . . .) materials in such devices [43]. Molecular species can however be used to enhance the catalytic properties of active materials. Coating of a platinum electrode with conducting polypyrrole containing ferrocene sulfonate as counter-ion or with polypyrrole covalently bound to [1.1]ferrocenophane indeed induces a 0.27 V anodic shift for proton reduction in molar sulfuric acid and a sevenfold amplification of current density when poised at −0.44 V/SHE [44]. In the same way, Kanedo et al. reported that modified platinum electrode coated with Nafion incorporating neutral [Co(TPP)] (**13**) display better proton reduction activity at pH 1 than a bare platinum electrode [41].

From the viewpoint of solar energy conversion however, the development of photocatalysts for overall water splitting is an attractive goal. Aside from composite semiconductor-based materials [45], homogeneous systems for hydrogen photoproduction consist in a photosensitizer S held in an excited state upon irradiation. This excited S^* then transfers electrons to a relay R able to effect proton reduction (Fig. 8). If solar energy is directly used to drive the catalytic hydrogen production cycle, larger overpotentials for proton reduction are acceptable. Indeed, photovoltaic conversion, which is still achieved with poor quantum yields, is avoided. This opens the field for the technological application of synthetic molecular catalysts. Water splitting indeed requires a voltage of 1.23 V, whereas the energy of visible light lies between 1.56 and 3.12 eV, which allows 0.33–1.89 V overvoltage shared between cathodic and anodic processes.

First generation photochemical systems for proton reduction successfully used photosensibilizers such as $[Ru(bipy)_3]^{2+}$ ($E^\circ([Ru(bipy)_3]^{2+*}/[Ru(bipy)_3]^{3+}) = -0.87$ V versus SHE) [46] or TiO_2 ($E_{1/2}(CB) = -0.11$–0.059 pH versus SHE) [47]. Reports of structural, but non-functional, mimics of hydrogenases covalently linked to a ruthenium polypyridine photosensitizer recently appeared in the literature [48].

A related application is photoelectrochemical production of hydrogen where the externally applied potential is reduced by a photogenerated potential. Polymer bound [1.1]ferrocenophane (**3′**), deposited on a p-type silicon photocathode, allows proton reduction in acidic aqueous solution with an underpotential of 300 mV, i.e. the proton reduction occurs at a potential 300 mV more positive than the standard apparent potential of the H^+/H_2 couple [27].

5.3. A good catalyst is a robust catalyst!

The crucial point for any technological application is the robustness of the catalyst, which means both thermodynamic and kinetic stability under normal atmospheric conditions and high turnover numbers. Up to now, all promising molecular chemical systems for proton reduction or hydrogen uptake have been abandoned because they were not reliable enough. The following points should be considered.

First, involvement of two electron transfers in the catalytic cycle implies that the selected catalysts, at the unprotonated or hydridic state (depending on the mechanism), should display electrochemically and chemically reversible (except for protonation/deprotonation or H_2 coordination/decoordination

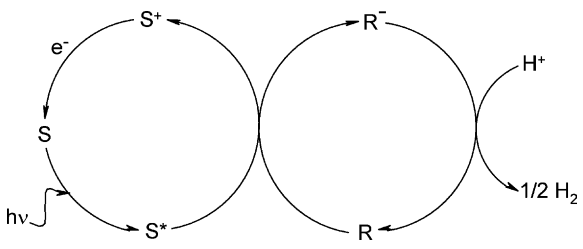

Fig. 8. Principles of photoinduced electrocatalytic reduction of protons.

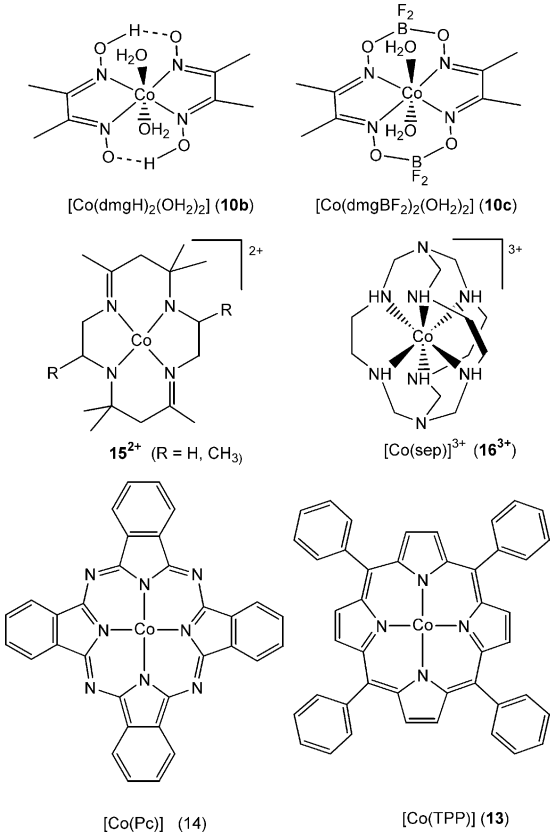

Fig. 9. Selected examples of synthetic cobalt catalysts stabilized by chelate effect.

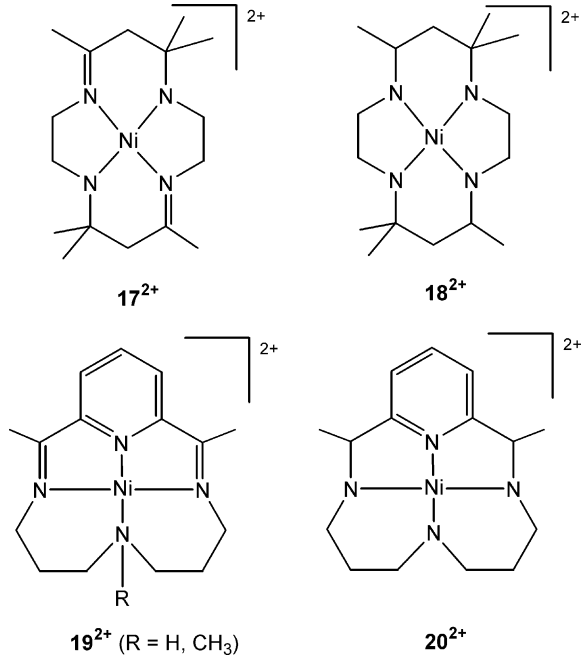

Fig. 10. Selected examples of synthetic nickel catalysts stabilized by chelate effect.

steps) redox features, occurring at relatively mild potential to avoid any irreversible ligand decomposition.

Second, the chelate effect has been widely used as a general strategy for the design of robust complexes [9]. By preventing ligand exchange in the active intermediate states, this indeed ensures conservation of the entire set of ligands, governing the reactivity of the metallic center, over the whole catalytic cycle.[2] Bidentate ligands such as dithiolene [49] or alkylglyoxime [22,46] have been extensively used. A large number of macrocyclic complexes of the metals belonging to the Fe, Co (Fig. 9) and Ni (Fig. 10) triads, including porphyrins [23–25,29,30,41], phtalocyanines [42], cyclams [28,50] or other polydentate ligands [34,51,52], have also been investigated. Cyclopentadienyl ligands, which have the property to stabilize both high and low oxidation states have been exploited, in conjunction with a bidentate ancillary ligand such as diphosphine [39,53], alkylglyoxime [54] or bipyridine [36,37,47]. The corresponding complexes (Fig. 11) usually have another exchangeable coordination site, to accommodate hydride, water or molecular hydrogen. This was mainly developed by Kölle et al., namely with cyclopentadienyl complexes of cobalt [52,53] and rhodium [36,37,47,54] and by Mueller-Westerhoff et al. and Bitterwolf et al. with binuclear organometallic complexes such as **3** [27].

Several complexes incorporating such chelating ligands allowed the design of stable and active electrocatalytic [23,37,41,42] or photoelectrocatalytic [27,46,47] materials.

Third, the catalyst should be resistant to hydrogenation or acidic hydrolysis. The cobaloxime $[Co(dmgH)_2(H_2O)_2]$ (**10b**), able to catalyze proton electroreduction at high rate with relatively low activation overpotential in neutral solution [55], unfortunately undergoes hydride transfer from the metal center to two oxime moieties, leading to an inactive bisoximatobishydroxylamino complex (Fig. 12) [46,56]. Coordination of a pyridine in axial position brings about a 200–300-fold increase in the ligand hydrogenation rate. Similar H atom transfer reactions from the intermediate hydride species are also supposed to account for the degradation of porphyrin complexes used for proton electroreduction [24]. Fortunately, this does not apply to all unsaturated carbon–heteroatom systems since no hydrogenation of the ligand was observed when complex $\mathbf{19}^{2+}$, which contains two imine functions, was used for electrocatalytic proton reduction [51].

Cobaloximes are also prone to demetalation in acidic media (pH < 5) (Fig. 12) [57]. Again, the chelate effect can help overcoming this degradation process since the BF_2-bridged analogue $[Co(dmgBF_2)_2(OH_2)_2]$ (**10c**) proved stable in acidic media [58].

[2] Note that the biomimetic approach could be in contradiction with this strategy since the carbonyl ligands, if conserved in biomimics, could be likely to irreversible displacement during catalysis (see for example the dimerization process initiated by CO displacement upon thiolate nucleophilic attack in the reduced $[Fe_2(\mu\text{-pdt})(CO)_6]^-$ [61h]). CO loss, when limited to a sole ligand can nevertheless be a convenient way of generating a vacant site at a metal center for substrate binding.

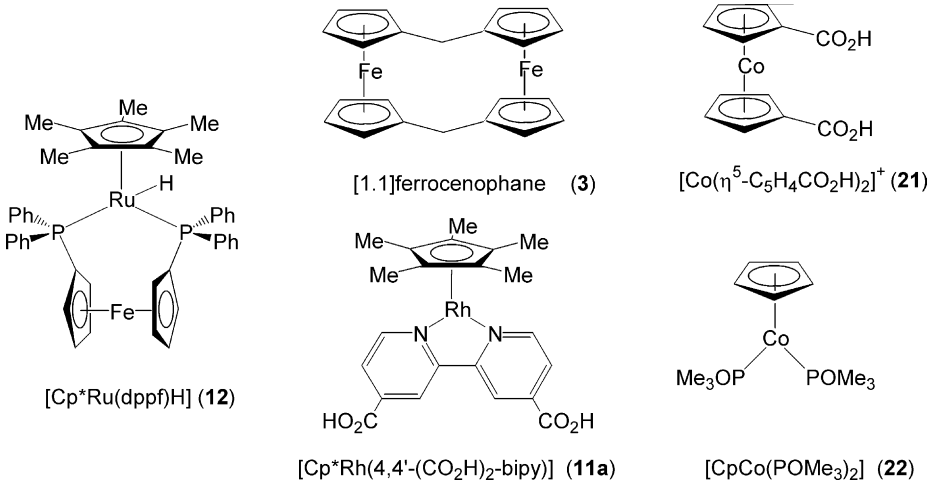

Fig. 11. Selected examples of synthetic organometallic catalysts.

6. Designing a catalyst, not so easy to do!

The de novo design of a catalyst for proton reduction or hydrogen oxidation is not an easy task considering all the parameters to accommodate. Potential guidelines could be found in the structural patterns observed at the active site of hydrogenases and responsible for their activity. Variation on the metal ion and its coordination sphere should also be used as a synthetic control of the reactivity to fulfill the electronic and structural requirements of each elementary step of the catalytic cycle.

6.1. Towards bio-inspired functional models

A purely biomimetic approach of [Fe]-only hydrogenases [6] has been exquisitely and successfully developed by the groups of Rauchfuss [59], Darensbourg [60] and Pickett [61]. The resulting model compounds have retained the sulfur environment, the nature and number of metal ions as well as the diatomic carbonyl and cyanide ligands found at the active site. Some of those compounds display promising activities [59b,60b,d,e]. These results are described in other articles in this issue. In our laboratory, we have initiated studies of catalysts, that we name bio-inspired catalysts, which do not necessarily contain altogether sulfur ligands, iron or nickel metal and diatomic ligands but are designed on the basis of considerations described below. We want herein to briefly describe and illustrate our approach from various literature results.

6.1.1. Sulfur-rich coordination sphere

Since the metals in the active sites of both [Fe]-only and [NiFe] hydrogenases are in a sulfur-rich environment, this has prompted the development of new metallic systems using

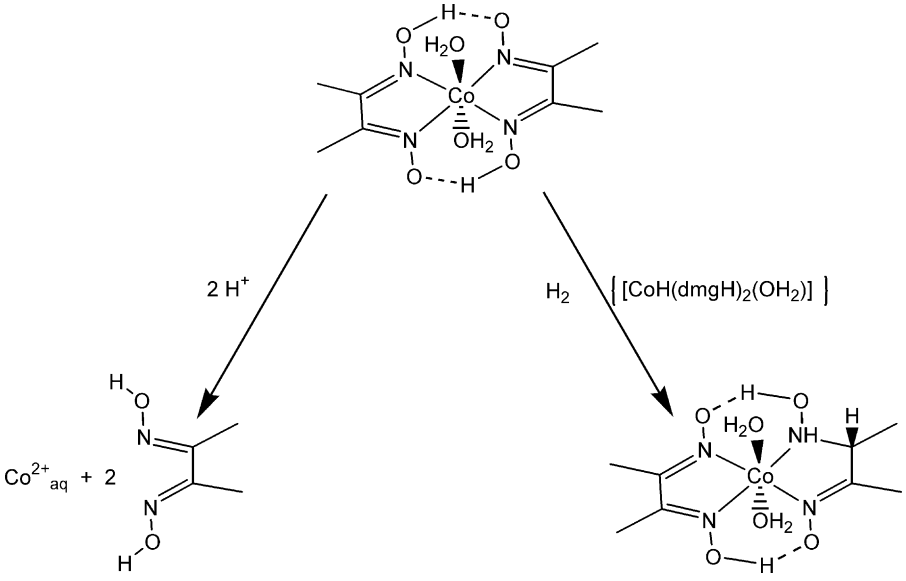

Fig. 12. Decomposition processes of $[Co(dmgH)_2(OH_2)_2]$ (**10b**).

macrocyclic sulfur-containing ligands. This field has been mainly pioneered by Sellmann et al. [8,35,49,62–64]. Since they can act as σ-donor, σ-donor π-acceptor or even σ-donor π-donor ligands, sulfide, thiolate and thioether can tune the electronic properties of the metal ions. The resulting complexes then display a remarkable electronic flexibility: they can accommodate both hard and soft ancillary ligands and show a rich, sometimes ligand-centered, chemistry.

One of the first systems displaying hydrogenase activity, assayed by H/D exchange, was a palladium complex **23** of the salen ligand [34]. It is thought that the heterolytic cleavage of hydrogen at the palladium–phenolate sites proceeds by metathesis of the palladium–phenolate bond. A nickel catalyst **24** with the same kind of activity but involving a nickel–thiolate bond (Fig. 13), was reported 25 years later by Sellmann et al. [62]. Coordination of the elaborated sulfur-rich tridentate ligand and of a distinct phosphinimine ligand confers to the first row transition nickel ion electronic properties, and hence reactivity, similar to those of the expensive palladium complex. This example highlights the capital contribution of organic sulfur chemistry for the elaboration of new bio-inspired electrocatalytic molecular materials in order to replace platinum electrocatalysts. Moreover, the activation overpotential of hydrogen evolution on the mercury electrode in the circumneutral pH-range is strongly diminished in the presence of nickel ions and cysteine or aminothiols [65].

6.1.2. Internal basic site

The second interesting feature of the active sites in both [Fe]-only and [NiFe] hydrogenases is the presence of an internal base near the metallic catalytic centers assisting deprotonation of the bound dihydrogen. On the basis of the three-dimensional structure of *D. desulfuricans* [Fe]-only hydrogenase, Fontecilla-Camps and co-workers pointed to the possibility for the presence of a nitrogen atom at the center of the five atom iron-bridging molecule, and modelized it as a dithiomethylamine rather than a propane-1,3-dithiolate (Fig. 1) [3]. The active site is nicely designed so that the basic center is kept far enough to avoid coordination to the metal ion. Such a configuration may indicate that the cleavage of dihydrogen proceeds via nucleophilic addition rather than oxidative addition or a four-center transition state mechanism (also called σ-bond metathesis) (Fig. 14) [66]. The cleavage of bound dihydrogen then relies on the polarization of the H_2 bond by the base B to form an activated complex displaying an unconventional hydrogen bond, $M–H^{\delta-}\cdots^{\delta+}H–B$, called dihydrogen bond [67]. This activated complex further evolves to a species containing a hydride ligand M–H and a protonated base B–H. The reverse reaction involves intramolecular proton transfer from B–H to M–H to generate a η^2-H_2 complex.

This hypothesis is strongly corroborated by theoretical models of [Fe]-only [68] and [NiFe] [69] hydrogenases (Fig. 15). In the case of [NiFe] and [NiFeSe] hydrogenases, dihydrogen is first coordinated to the iron atom and the sulfur atom of a terminal cysteine (respectively selenocysteine) bound to the nickel ion is thought to play the role of a base.

It is interesting to note that chemical systems containing both a hydride metal center and a weak acid/base residue held by an ancillary ligand such as [Ni(*o*-

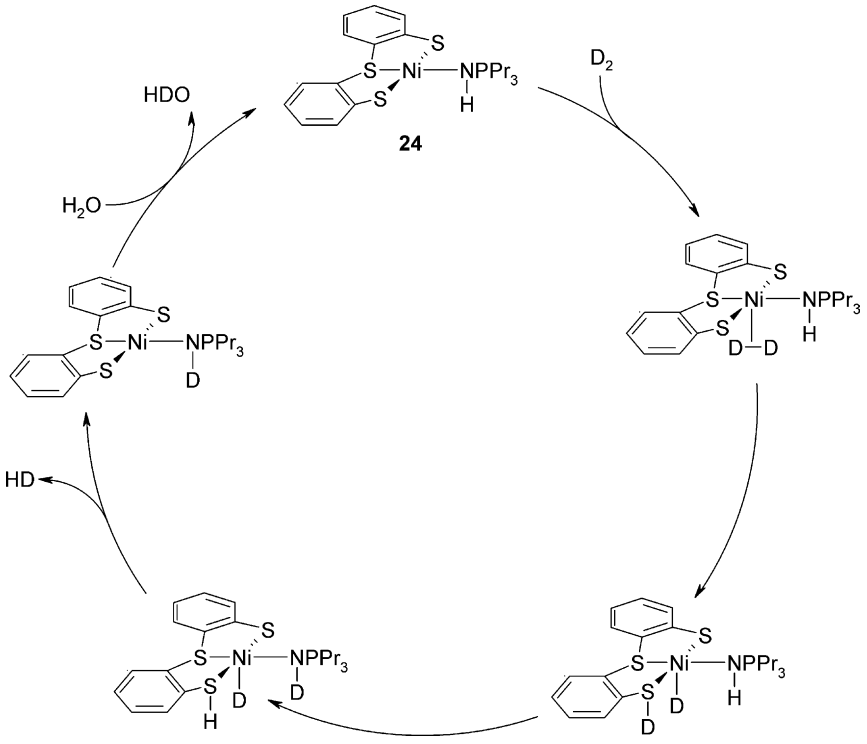

Fig. 13. Mechanism of the [Ni(NHP^{n}Pr$_3$)(S$_3$)] (**24**) catalyzed D_2/H^+ exchange.

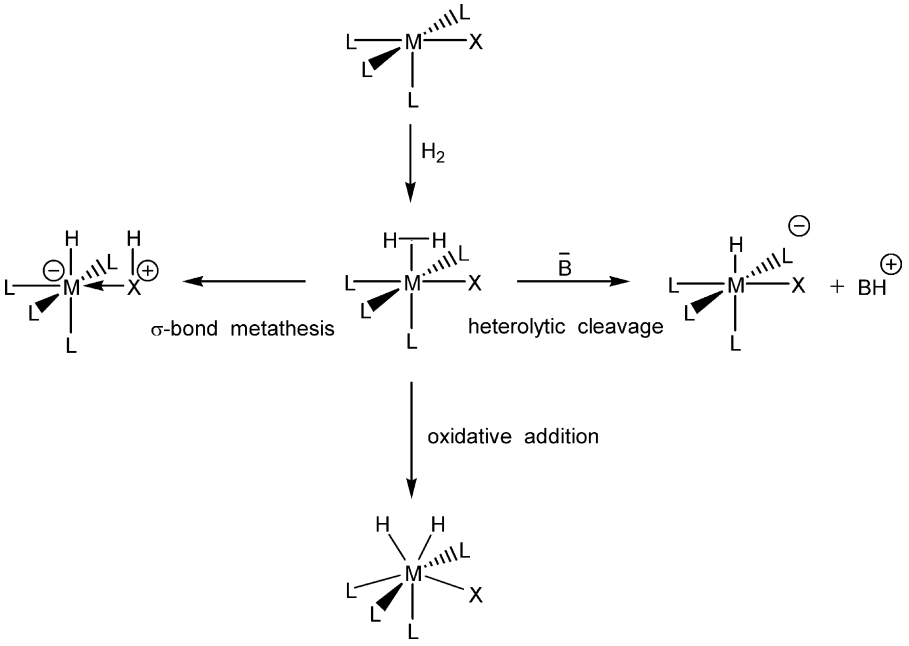

Fig. 14. Mechanisms for homolytic and heterolytic dihydrogen activation.

$C_6H_4(OH)CH{=}N{-}NHCSNH_2)_2$] [70], $[Ir(L)(PPh_3)_2(H)_2)]^+$ (L = iminol tautomer of quinoline-8-acetamide (**25**$^+$) [71a] or cyclometalated 2-ammonium-7,8-benzoquinolinato (**26**$^+$) [71b]), $[Ir(H)_3(2\text{-}C_6H_4NH_2)(PPh_3)_2)]^+$ (**27**$^+$) [71c], $[Ir\{H(\eta^1\text{-}SC_5H_4NH)\}_2(PCy_3)_2]^+$ (**28**$^+$) [71de], $[Cp^*W(OH)(\mu\text{-}S)_2RuH(PPh_3)_2]^+$ (**29**$^+$) [72], $[\eta^5\text{-}C_5H_4(CH_2)_3NMe_2H)RuH(dppm)]^+$ (**30a**$^+$) [73] or Jalón complex **31** [74] have H/D exchange activity (Fig. 16), some of those systems displaying a dihydrogen bond. For example, when a solution of **31** in CD_3OD is exposed to a dihydrogen atmosphere at room temperature and 1 atm, more than 90% of H_2 is exchanged for D_2 in about half an hour. The heterolytic splitting of the dihydrogen ligand in **30a**$^+$ is believed to be the crucial step to explain its catalytic activity for the reduction of CO_2 into formic acid. Similarly, the presence of an electronically coupled acidic OH or NH group and a ruthenium hydride in the same molecule is the key to the high reactivity of the catalysts of Shvo [75], Casey [76] and Noyori [77] for the hydrogenation of aldehydes, ketones and imines.

NMR measurements indicated the existence of an intramolecular N–H···H–Ru hydrogen bonding interaction in

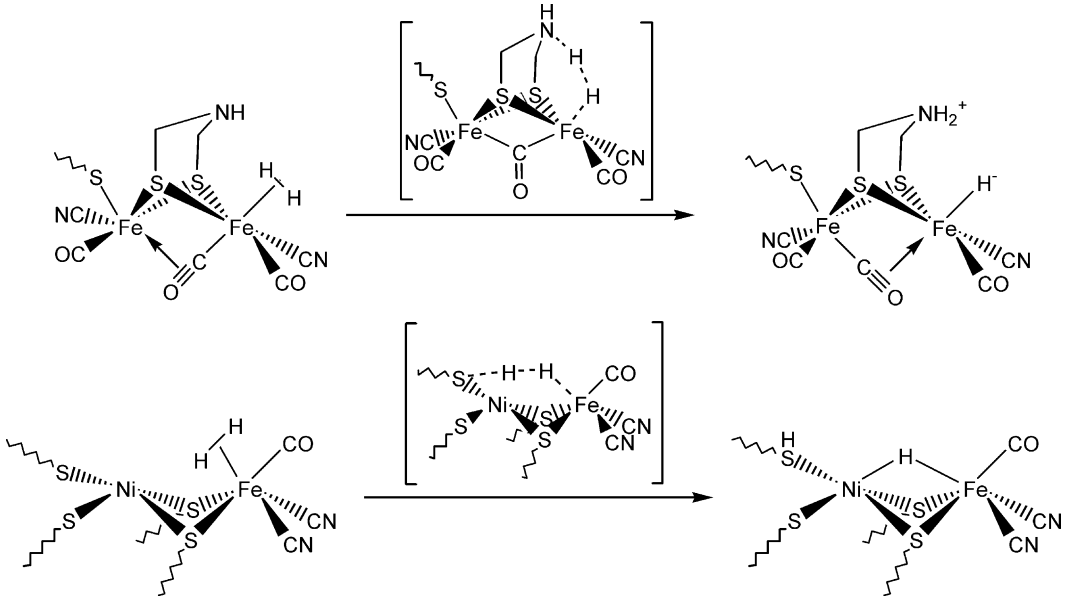

Fig. 15. Heterolytic cleavage of hydrogen along a nucleophilic addition pathway for [Fe]-only and [NiFe] hydrogenases.

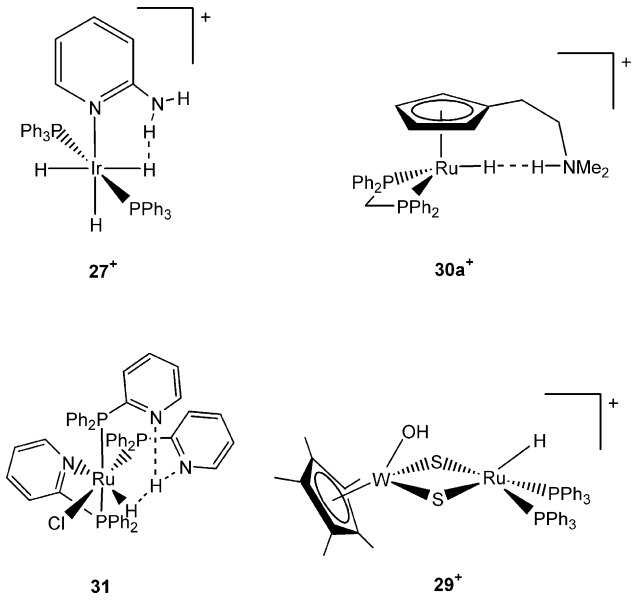

Fig. 16. Selected H^+/H^--containing systems.

$[\eta^5\text{-}C_5H_4(CH_2)_3NMe_2H)RuH(L)]^+$ (L = dppm (**30a**$^+$) [73], 2 PPh_3 (**30b**$^+$) [78]), probably implicated in the fast exchange between the hydride ligand and N–H. In $[\eta^5\text{-}C_5H_4(CH_2)_3NMe_2)Ru(dppm)]^+$ however, the pendant amino residue can coordinate the ruthenium atom, so that a pressure of 60 atmospheres of hydrogen is necessary to form **30a**$^+$. Hence, a good activity for hydrogen oxidation or proton reduction depends on the fact that the base does not coordinate the metal ion, as it is the case in the active site of [Fe]-only hydrogenase. Such a goal is achieved in the ingenious system recently described by DuBois and co-workers [31] (Fig. 7) which combines a tetraphosphino-nickel core known to promote the heterolytic cleavage of hydrogen and an internal nitrogen base related to the dithiomethylamine cofactor of [Fe]-only hydrogenases. Remarkably, the presence of the nitrogen atom in the ligand induces a decrease of 600 mV for the oxidation potential of $[HNi\{(Et_2PCH_2)_2NMe\}_2]^+$ (**9H**$^+$) compared to the parent $[HNi(depp)_2]^+$. This drastic shift in potential can be explained by a coupling of the oxidation process of the hydride complex with a rapid proton transfer from Ni to the base N atom and ultimately to the solution. A similar 230 mV decrease of the reduction potential of protons in acetonitrile catalyzed by the biomimetic hexacarbonyl diiron clusters seems to occur when switching from the propane-1,3-dithiolate [59b] to the N-aryl-2-aza-propane-1,3-dithiolate [79] bridge, provided the fact that the different experimental conditions, namely the nature of added acid, do not modify the nature of the electrocatalytic process.

The H/D exchange activity of $[Ir(H)_2(HS(CH_2)_3SH)(PCy_3)_2]^+$ (**32**$^+$) [80], $[Ru(py^{bu}S_4)]_2$ (**33**) [81], $[RhH(^{bu}S_4)(CO)]$ (**34**) [63a], $[OsH(py^{bu}S_4)]^-$ [63b] or $[Ni(NHP^nPr_3)(S_3)]$ (**24**) [62] (Fig. 13) is also attributed to the existence of a Lewis-acidic metal together with thiolate donors as "built-in" bases (Fig. 17). In these cases, the thiolate base is coordinated to the metal ion, the complex possessing another vacant site to accommodate a dihydrogen molecule or a hydride ligand, and it is not easy to define whether the activity relies on a four-center transition state mechanism or a nucleophilic addition pathway.

Another class of systems able to promote stoichiometric or catalytic heterolytic hydrogen cleavage consists of mononuclear or binuclear complexes such as **35** and **36** (Fig. 17)

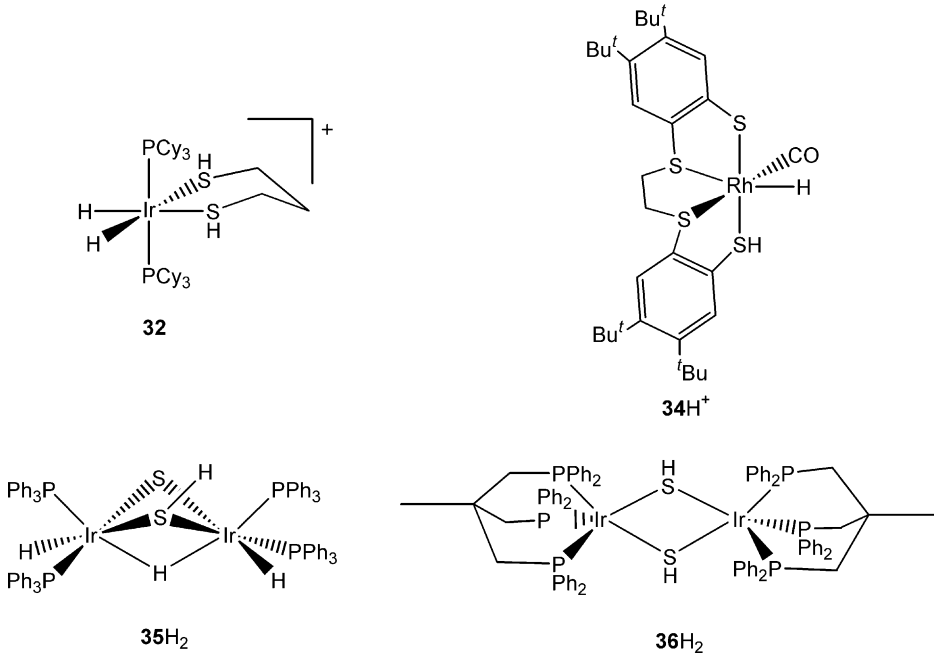

Fig. 17. Selected catalysts for heterolytic hydrogen cleavage containing thiolate or sulfide as "built-in" bases.

containing terminal or bridged sulfide as "built-in" bases [82].

6.1.3. Binuclearity

The observation of binuclear clusters at both, although significantly different, active sites of [Fe]-only and [NiFe] hydrogenases raises the issue whether two metal ions are essential to achieve heterolytic formation or cleavage of hydrogen (it was outlined above than two metal centers are required for the corresponding homolytic reactions). There are two interdependent issues regarding binuclearity: (i) the storage of one redox equivalent on each metal center instead of both redox equivalents on the same ion can help keeping the potential features of the cluster near the H^+/H_2 couple potential; (ii) intermediates can be stabilized (hydride species) or activated (coordinated dihydrogen) in a bridging coordination mode.

The last hypothesis still derives from stereochemical considerations based on the crystallographic structures and are not ascertained by experimental measurements on enzymes or biomimics. Most of the different quantum chemical calculations on [NiFe] hydrogenases, however, conclude that the heterolytic cleavage of hydrogen, initially bound to the iron or the nickel ion, results in a hydride ligand bridging between the two metal centers and a protonated terminal cysteine residue (Fig. 15) [69]. On the other hand, bridging hydride are recurrent in transition metal cluster chemistry [83] and the M–H–M bond displays a peculiar three centers–two electrons electronic structure with a substantial amount of metal–metal bonding. Moreover, few model reactions for heterolytic cleavage of dihydrogen are known. Amazingly, and although this was expected neither from the crystallographic structures nor from quantum calculations for [Fe]-only hydrogenases, the biomimetic $\{Fe^I\}_2$ models of these enzymes, $[(\mu\text{-pdt})\{Fe(CO)_2(L)\}_2]$ (pdt = $S(CH_2)_3S$; L = CO, CN^-, PMe_3), yield the bridging hydride species $[(\mu\text{-pdt})(\mu\text{-H})\{Fe(CO)_2(L)\}_2]^+$ upon protonation [59b,60b–e]. $[(\mu\text{-pdt})(\mu\text{-H})\{Fe(CO)_2(PMe_3)\}_2]^+$ is even able to catalyze H/D exchange via H_2 heterolytic cleavage under sunlight exposition [60b]. Other model reactions involving hydride bridged polynuclear species include the hydrogenation of organometallic iridium $[(\mu\text{-}S)_2\{IrH(PPh_3)_2\}_2]$ (**35**) [82c] or $[Cp^*Ir(OH_2)_3]^{2+}$ [84], and ruthenium, $[(C_6Me_6)Ru(OH_2)_3]^{2+}$ or $[(arene)RuCl_2]_2$ (arene = C_6H_6, $C_6H_2Me_4$), complexes [85].

Hence, studies on model reactions of the heterolytic dihydrogen activation/formation on dinuclear metal centers are more than ever relevant to provide a clue about the requirement of binuclearity for biological proton reduction or hydrogen oxidation.

6.2. Tuning the reactivity of the metal center

The achievement of high turnover frequencies relies on the absence of any bottleneck along the catalytic pathway, i.e. each elementary step should process spontaneously and rapidly. Varying the ligands and the nature or oxidation state of the metal center, with regard to their hard/soft features, *trans* effect or steric crowding, modifies the reactivity of the metal center and orientates each step in one or the other direction.

The key steps of the catalytic process are those involving proton transfer, namely the H_2 cleavage and the resulting hydride deprotonation and the reverse reactions, hydride protonation, dihydrogen reductive elimination and metal protonation. The chemistry of transition metal dihydrogen complexes has been reviewed by Jessop and Morris [86].

6.2.1. Dihydrogen coordination

Apart from the fact that the catalyst should display a vacant or labile coordination position, coordination of dihydrogen [71e] requires electron density on the metal, which enhance π-retrodonation into the antibonding orbitals of dihydrogen. Too little retrodonation leads to short-lived metal–dihydrogen complexes which thus cannot be deprotonated. On the opposite, too much π-donation results in a metal–dihydrogen species with a strong dihydridic nature and thus difficult to deprotonate. Displacement of a dihydrogen molecule is easier for the harder metals of the first and second transition metal series [87]. Morris has developed an original approach [86,88] for predicting the properties of η^2-dihydrogen complexes $[M(H_2)L_5]$ based on the determination of the electrochemical potential $E_{1/2}(d^5/d^6)$ of the corresponding dinitrogen complexes $[M(N_2)L_5]$ using the additive electrochemical parameters for the ligand set and Lever's correlations for transition metal of groups 6–8 [89]. If $E_{1/2}(d^5/d^6) < 0.0$ to 0.5 V/SHE (depending on the transition series), the complex will undergo oxidative addition to yield a dihydride species. Below 1.7–2.0 V/SHE, the dihydrogen complex is stable toward loss of H_2 whereas above 1.7–2.0 V/SHE, decoordination of H_2 occurs at 25 °C.

6.2.2. Hydrogen heterolytic cleavage

Such a process is in competition with oxidative addition of bound dihydrogen to give a dihydride species. Kinetic experiments on mixtures of $[Ru(H_2)CpL]^+$ and $[Ru(H)_2CpL]^+$ (L = dtfpe, dppe, dape) showed that the dihydrogen complex is deprotonated faster than the dihydride compound [90]. In a catalytic process, the heterolytic pathway is then preferable. Oxidative addition can be avoided by (i) controlling the electronic properties of the coordination sphere (see above) and (ii) releasing the steric crowding around the coordinated dihydrogen ligand. Two mechanisms are then possible (Fig. 14): (i) deprotonation of η^2-H_2 by a base, which can be external (intermolecular H^+ transfer) or internal (i.e. a ligand lone pair) or (ii) protonation of a metal–ligand bond (four-center transition state mechanism). The former mechanism requires an acidic η^2-H_2 ligand. Morris calculated that the most acidic dihydrogen complexes are also the less stable toward H_2 loss, i.e. the corresponding $[M(N_2)L_5]$ complexes have $E_{1/2}(d^5/d^6) > 2.0$/SHE. Nevertheless, stable H_2 complexes have pK_a values ranging from −9 to 34, the lower

$E_{1/2}$ value (i.e. the greater electron density at the metal), the lower acidity.

6.2.3. Hydride protonation

Werner could demonstrate that hydridicity, i.e. reaction with a proton, of a hydride species is favored by hard ancillary ligands since this reaction corresponds to an increase of the net positive charge of the complex [87]. The hydridicity is also strongly increased when the oxidation state of the metal decreases: $[Rh^{II}H(TPP)]^-$ (**8H**$^-$) catalyses proton electroreduction via the heterolytic pathway whereas $[Rh^{III}H(TPP)]$ (**8H**) is inactive (Fig. 18) [30].

Axial ligation *trans* to the hydride ligand also affects the hydridicity: the rhodium porphyrin species $[Rh^{I}(TPP)]^-$ (**8**$^-$) can be protonated to give **8H** but this hydride doesn't react with a proton to eliminate a dihydrogen molecule. Binding of triethylphosphine to rhodium increases electron density on the hydrogen atom bound to rhodium and $[Rh^{III}H(TPP)(PEt_3)]$ catalyzes proton electroreduction (Fig. 18) [30].

6.2.4. Reductive elimination

The weaker the M–H bond, the easier reductive elimination of hydrogen from two metal hydride species. The stability of a metal hydride is strongly influenced by the metallic oxidation state: ruthenium(III) porphyrin hydrides easily eliminate dihydrogen while the anionic ruthenium(II) hydrides are resistant to reductive elimination [25c]. Since this requires that the two species come into contact, the reaction can be prevented by steric or Coulombic repulsions or favored in dinuclear catalysts such as [1.1]ferrocenophane (**3**) [27].

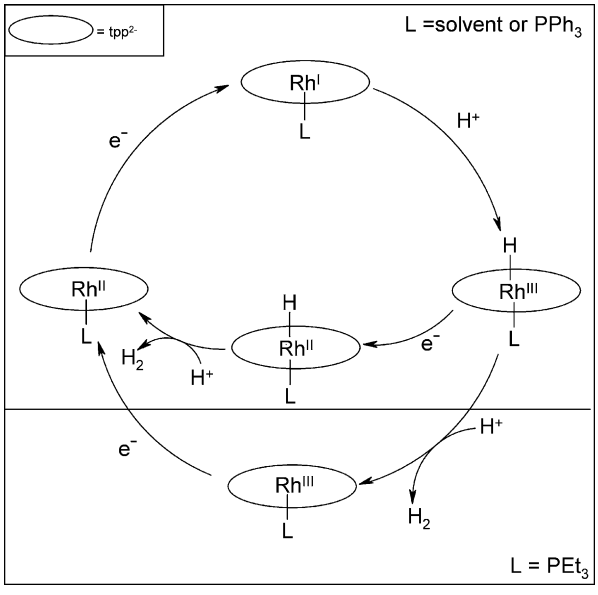

Fig. 18. Simplified mechanism for proton reduction catalyzed by $[Rh(TPP)]^-$ (**8**$^-$) (dissociation steps of axial ligands other than H^- have been omitted for clarity and global charges of the species are not indicated).

6.2.5. Metal protonation/hydride deprotonation

Werner has pointed out the influence of the ancillary ligand set L_n on the acidity of hydride ligands. Considering Eq. (6), it is indeed easy to predict that hard bases will stabilize the HML_n form, while soft bases will stabilize ML_n^- [87]. Note that the pK_a of hydride complexes strongly depends on the oxidation state of the metal center: the pK_a of $[HCo(dppe)_2]$ decreases by 14.5 units upon oxidation [91]. The influence of the metal is somewhat more complicated since the hydrides of the second transition series seem to be less acidic than those of the first series for the metals to the left in the periodic table but more acidic to the right, iron and ruthenium lying at the borderline. The hydrides of the third series are the weakest acids [87].

$$[HML_n] \rightleftharpoons [ML_n]^- + H^+ \quad (6)$$

6.2.6. Structural distortions

DuBois and co-workers have pointed out the fundamental effects of the tetrahedral distortion of nickel complexes on their hydride acceptor ability. The hydride acceptor ability of the largely tetrahedral deformed $[Ni\{(Et_2PCH_2)_2NBu\}_2]^{2+}$ (**9**$^{2+}$) increases by 10 kcal mol^{-1} compared to the nearly square planar $[Ni\{(Et_2PCH_2)_2NMe\}_2(dmpm)](BF_4)_2$ [31]. In a systematic study on palladium bisdiphosphine complexes, DuBois and co-workers also demonstrated that hydridicity strongly depends on structural distortions induced by the natural bite angle of the ligands [92]. Such a tetrahedral distortion is also observed at the active site of [NiFe] hydrogenases, perhaps with the same effects.

6.3. Decreasing overpotentials

The hardness or softness properties of the coordination sphere do influence not only the protonation/deprotonation steps but also the redox processes. Unfortunately, both effects are opposed for a given catalytic cycle: for proton reduction, hard ligands enhance the protonation of low-valent metal ions and hydridicity of metal hydride moieties but decrease the potentials of the reduction steps. They accelerate the reaction but increase the overpotential. The same applies for hydrogen oxidation: the harder the ancillary ligand set, the lower the oxidation potentials, while soft or electron rich ligands are needed to promote hydrogen cleavage.

Several studies have been undertaken in order to control the reduction potential of the catalyst by systematically varying central metals and axial ligands in porphyrin complexes [25b] or equatorial and axial ligands in cobaloximes. As a conclusion of these studies, it was stressed that "modification of the reduction potentials of a closely related set of catalysts, i.e. varying remote substituents of the ligands, results in insignificant changes in the overpotential for proton reduction". The species with a relatively positive reduction potential are less nucleophilic and then exhibit catalytic activity only under strongly acidic conditions. As an example, 330 mV are gained in reduction potential when substituting

glyoximato (gH^-) for dimethylglyoximato ($dmgH^-$) in $[Co^{II}(dmgH)_2(py)]$ [55], but $[Co(gH)_2(PBu_3)]^-$ is approximately 600 times less nucleophilic than $[Co(dmgH)_2(PBu_3]^-$ [93]. Hence, more radical changes, such as varying the metal ion or the nature of some ligands or modifying the structure of the catalyst, are needed to minimize the working overpotential.

7. Conclusion

In the current context of sustainable development, the design of economically viable molecular catalysts for proton reduction and hydrogen oxidation are more than ever crucial challenges for synthetic chemists. The reported electrocatalysts for proton reduction display high turnover frequencies and total turnover numbers but their working overpotentials are still too large compared to the composite materials currently used in electrochemical devices. For hydrogen oxidation, a few complexes able to promote heterolytic hydrogen cleavage, among them only two electrocatalysts, are reported. The design of a new catalyst for hydrogen oxidation is then closely related to the development of new systems for stoichiometric heterolytic hydrogen oxidation, perhaps inspired from the nature. However, up to now, the increasing amount of crystallographic structures of enzymes delivered by post-genomic programs may have led the chemist astray in a rigorous structural modelization of the active sites of the enzymes instead of carefully analyzing these structures and picking up the fundamental features responsible for the activity of the bioactive clusters. In the future, it is likely that functional models will be bio-inspired complexes rather than atomic models.

References

[1] J.A. Turner, Science 285 (1999) 687.
[2] M.W.W. Adams, L.E. Mortenson, J.-S. Chen, Biochim. Biophys. Acta 594 (1981) 105;
P.M. Vignais, B. Billoud, J. Meyer, FEMS Microbiol. Rev. 25 (2001) 455.
[3] [Fe]-only hydrogenases: J.W. Peters, W.N. Lanzilotta, B.J. Lemon, L.C. Seefeldt, Science 282 (1998) 1853;
Y. Nicolet, C. Piras, P. Legrand, C.E. Hatchikian, J.C. Fontecilla-Camps, Structure 7 (1999) 13;
[NiFe] hydrogenases: A. Volbeda, M.H. Charon, C. Piras, E.C. Hatchikian, M. Frey, J.C. Fontecilla-Camps, Nature 373 (1995) 580;
A. Volbeda, E. Garcin, C. Piras, A.L. de Lacey, V.M. Fernandez, E.C. Hatchikian, M. Frey, J.C. Fontecilla-Camps, J. Am. Chem. Soc. 118 (1996) 12989;
Y. Higuchi, T. Yagi, N. Yasuoka, Structure 5 (1997) 1671;
Y. Higuchi, H. Ogata, K. Miki, N. Yasuoka, T. Yagi, Structure 7 (1999) 549.
[4] A.K. Jones, E. Sillery, S.P.J. Albracht, F.A. Armstrong, Chem. Commun. (2002) 866.
[5] M.Y. Darensbourg, E.J. Lyon, J.J. Smee, Coord. Chem. Rev. 206–207 (2000) 533;
A.C. Marr, D.J.E. Spencer, M. Schröder, Coord. Chem. Rev. 219–221 (2001) 1055.
[6] J. Alper, Science 299 (2003) 1686.
[7] J.A. Ibers, R.H. Holm, Science 209 (1980) 223.
[8] D. Sellmann, J. Sutter, Acc. Chem. Res. 30 (1997) 460.
[9] U. Kölle, New J. Chem. 16 (1992) 157.
[10] S.P.J. Albracht, Biochim. Biophys. Acta 1188 (1994) 167.
[11] H.R. Pershad, J.L.C. Duff, H.A. Heering, E.C. Duin, S.P.J. Albracht, F.A. Armstrong, Biochemistry 38 (1999) 8992;
C. Léger, A.K. Jones, W. Roseboom, S.P.J. Albracht, F.A. Armstrong, Biochemistry 41 (2002) 15736;
S.E. Lamle, K.A. Vincent, L.M. Halliwell, S.P.J. Albracht, F.A. Armstrong, Dalton Trans. (2003) 4152.
[12] S.V. Morozov, E.E. Karyakina, N.A. Zorin, S.D. Varfolomeyev, S. Cosnier, A.A. Kyryakin, Bioelectrochemistry 55 (2002) 169.
[13] J.N. Butt, M. Filipiak, W.R. Hagen, Eur. J. Biochem. 245 (1997) 116;
M. Guiral-Brugna, M.-T. Giudici-Orticoni, M. Bruschi, P. Bianco, J. Electroanal. Chem. 510 (2001) 136.
[14] C. Van Dijk, H.J. Grande, S.G. Mayhew, C. Veeger, Eur. J. Biochem. 107 (1980) 251.
[15] A.K. Jones, S.E. Lamle, H.R. Pershad, K.A. Vincent, S.P.J. Albracht, F.A. Armstrong, J. Am. Chem. Soc. 125 (2003) 8505.
[16] A.L. de Lacey, E.C. Hatchikian, A. Volbeda, M. Frey, J.C. Fontecilla-Camps, J. Am. Chem. Soc. 119 (1997) 7181.
[17] S.P.J. Albracht, Biochim. Biophys. Acta 1119 (1992) 148.
[18] A.I. Krashna, Enzyme Microb. Technol. 1 (1979) 165.
[19] N. Tamiya, S.L. Miller, J. Biol. Chem. 238 (1963) 2194.
[20] See, for example, P.M. Vignais, B. Dimon, N.A. Zorin, M. Tomiyama, A. Colbeau, J. Bacteriol. 182 (2000) 5997.
[21] D.D.M. Wayner, V.D. Parker, Acc. Chem. Res. 26 (1993) 287;
V.D. Parker, J. Am. Chem. Soc. 114 (1992) 7458.
[22] T.-H. Chao, J.H. Espenson, J. Am. Chem. Soc. 100 (1978) 129;
P. Connolly, J.H. Espenson, Inorg. Chem. 25 (1986) 2684.
[23] R.M. Kellet, T.G. Spiro, Inorg. Chem. 24 (1985) 2373;
R.M. Kellet, T.G. Spiro, Inorg. Chem. 24 (1985) 2378.
[24] J.P. Collman, P.S. Wagenknecht, N.S. Lewis, J. Am. Chem. Soc. 114 (1992) 5665.
[25] (a) J.P. Collman, P.S. Wagenknecht, J.E. Hutchison, Angew. Chem., Int. Ed. Engl. 33 (1994) 1537;
(b) J.P. Collman, Y. Ha, P.S. Wagenknecht, M.-A. Lopez, R. Guilard, J. Am. Chem. Soc. 115 (1993) 9080;
(c) J.P. Collman, J.E. Hutchison, P.S. Wagenknecht, N.S. Lewis, M.A. Lopez, R. Guilard, J. Am. Chem. Soc. 112 (1990) 8206;
J.P. Collman, P.S. Wagenknecht, J.E. Hutchison, N.S. Lewis, M.A. Lopez, R. Guilard, M. L'Her, A.A. Bothner-By, P.K. Mishra, J. Am. Chem. Soc. 114 (1992) 5654.
[26] T.E. Bitterwolf, A.C. Ling, J. Organomet. Chem. 57 (1973) C15;
T.E. Bitterwolf, A.C. Ling, J. Organomet. Chem. 215 (1981) 77;
T.E. Bitterwolf, J. Organomet. Chem. 252 (1983) 305;
T.E. Bitterwolf, W.C. Spink, M.D. Rausch, J. Organomet. Chem. 363 (1989) 189.
[27] U.T. Mueller-Westerhoff, A. Nazzal, J. Am. Chem. Soc. 106 (1984) 5381;
US patent 4,379,740 (12 April 1983).
[28] J.-P. Collin, A. Jouaiti, J.-P. Sauvage, Inorg. Chem. 27 (1988) 1986.
[29] I. Bhugun, D. Lexa, J.-M. Savéant, J. Am. Chem. Soc. 118 (1996) 3982.
[30] V. Grass, D. Lexa, J.-M. Savéant, J. Am. Chem. Soc. 119 (1997) 7526.
[31] C.J. Curtis, A. Miedaner, R. Ciancanelli, W.W. Ellis, B.C. Noll, M.R. DuBois, D.L. DuBois, Inorg. Chem. 42 (2003) 216.
[32] A. Deronzier, J.-C. Moutet, in: J.A. McCleverty, T.J. Meyer (Eds.), Comprehensive Coordination Chemistry II, vol. 9, Elsevier, Oxford, 2004, p. 471.
[33] P.A. Loach, in: G.D. Fastman (Ed.), Handbook of Biochemistry and Molecular Biology, vol. 1, third ed., C.R.C. Press, Inc., Cleveland, 1976, p. 122.
[34] G. Henrici-Olivé, S. Olivé, J. Mol. Catal. 1 (1975–1976) 121.

[35] D. Sellman, A. Fürsattel, Angew. Chem. Int. Ed. 38 (1999) 2023.
[36] U. Kölle, B.-S. Kang, P. Infelta, P. Comte, M. Grätzel, Chem. Ber. 122 (1989) 1869.
[37] S. Cosnier, A. Deronzier, N. Vlachopoulos, J. Chem. Soc., Chem. Commun. (1989) 1259.
[38] A.E. Kaifer, A.J. Bard, J. Phys. Chem. 89 (1985) 4876.
[39] R.T. Hembre, J.S. McQueen, V.W. Day, J. Am. Chem. Soc. 118 (1996) 798.
[40] V. Artero, M. Fontecave, unpublished results.
[41] T. Abe, F. Taguchi, H. Imaya, F. Zhao, J. Zhang, M. Kanedo, Polym. Adv. Technol. 9 (1998) 559.
[42] F. Zhao, J. Zhang, T. Abe, D. Wöhrle, M. Kanedo, J. Mol. Catal. (A) 145 (1999) 245.
[43] G.J.K. Acres, J.C. Frost, G.A. Hards, R.J. Potter, T.R. Ralph, D. Thompsett, G.T. Burstein, G.J. Hutchings, Catal. Today 38 (1997) 393;
P.M. Urban, A. Funke, J.T. Müller, M. Himmen, A. Docter, Appl. Catal. A 221 (2001) 459;
J. Divisek, H. Schmitz, B. Steffen, Electrochim. Acta 39 (1994) 1723;
M. Sadakane, E. Steckhan, Chem. Rev. 98 (1998) 219.
[44] J. Chen, J. Huang, G.F. Swiegers, C.O. Too, G.G. Wallace, Chem. Commun. (2004) 308.
[45] T. Takata, A. Tanaka, M. Hara, J.N. Kondo, K. Domen, Catal. Today 44 (1998) 17;
S. Licht, B. Wang, S. Mukerji, T. Soga, M. Umeno, H. Tributsch, Int. J. Hydrogen Energy 26 (2001) 653;
M. Hara, J. Nunoshige, T. Takata, J.N. Kondo, K. Domen, Chem. Commun. (2003) 3000.
[46] J. Hawecker, J.-M. Lehn, R. Ziessel, Nouv. J. Chim. 7 (1983) 271; M. Kirch, J.-M. Lehn, J.-P. Sauvage, Helv. Chim. Acta 62 (1979) 1345.
[47] U. Kölle, M. Grützel, Angew. Chem., Int. Ed. Engl. 26 (1987) 567.
[48] S. Ott, M. Kritikos, B. Akermark, L. Sun, Angew. Chem. Int. Ed. 42 (2003) 3285;
H. Wolpher, M. Borgström, L. Hammarström, J. Bergquist, V. Sundström, S. Styring, L. Sun, B. Akermark, Inorg. Chem. Commun. 6 (2003) 989.
[49] D. Sellmann, M. Geck, M. Moll, J. Am. Chem. Soc. 113 (1991) 5259.
[50] B. Fisher, R. Eisenberg, J. Am. Chem. Soc. 102 (1980) 7361.
[51] L.L. Efros, H.H. Thorp, G.W. Brudvig, R.H. Crabtree, Inorg. Chem. 31 (1992) 1722.
[52] V. Houlding, T. Geiger, U. Kölle, M. Grätzel, J. Chem. Soc., Chem. Commun. (1982) 681.
[53] U. Kölle, S. Ohst, Inorg. Chem. 25 (1986) 2689.
[54] U. Kölle, E. Raabe, C. Krüger, F.P. Rotzinger, Chem. Ber. 120 (1987) 979.
[55] M. Razavet, V. Artero, M. Fontecave, submitted for publication.
[56] L.I. Simandi, Z. Szeverényi, E. Budo-Zahonyi, Inorg. Nucl. Chem. Lett. 11 (1975) 773.
[57] A. Adin, J.H. Espenson, Inorg. Chem. 11 (1972) 686;
H.G. Gjerde, J.H. Espenson, Organometallics 1 (1982) 435.
[58] A. Bakac, J.H. Espenson, J. Am. Chem. Soc. 106 (1984) 5197;
K.A. Lance, K.A. Goldsby, D.H. Busch, Inorg. Chem. 29 (1990) 4537.
[59] (a) M. Schmidt, S.M. Contakes, T.B. Rauchfuss, J. Am. Chem. Soc. 121 (1999) 9736;
F. Gloaguen, J.D. Lawrence, M. Schmidt, S.R. Wilson, T.B. Rauchfuss, J. Am. Chem. Soc. 123 (2001) 12518;
(b) F. Gloaguen, J.D. Lawrence, T.B. Rauchfuss, J. Am. Chem. Soc. 123 (2001) 9476;
F. Gloaguen, J.D. Lawrence, T.B. Rauchfuss, M. Bénard, M.-M. Rohmer, Inorg. Chem. 41 (2002) 6573;
(c) J.D. Lawrence, H. Li, T.B. Rauchfuss, M. Bénard, M.-M. Rohmer, Angew. Chem. Int. Ed. 40 (2001) 1768;
J.D. Lawrence, H. Li, T.B. Rauchfuss, Chem. Commun. (2001) 1482;
H. Li, T.B. Rauchfuss, J. Am. Chem. Soc. 124 (2002) 726;
(d) J.D. Lawrence, T.B. Rauchfuss, S.R. Wilson, Inorg. Chem. 41 (2002) 6193.
[60] (a) E.J. Lyon, I.P. Georgakaki, J.H. Reibenspies, M.Y. Darensbourg, J. Am. Chem. Soc. 123 (2001) 3268;
M.Y. Darensbourg, E.J. Lyon, X. Zhao, I.P. Georgakaki, Proc. Natl. Acad. Sci. U.S.A. 100 (2003) 3683;
I.P. Georgakaki, L.M. Thomson, E.J. Lyon, M.B. Hall, M.Y. Darensbourg, Coord. Chem. Rev. 238–239 (2003) 255;
(b) X. Zhao, I.P. Georgakaki, M.L. Miller, J.C. Yarbrough, M.Y. Darensbourg, J. Am. Chem. Soc. 123 (2001) 9710;
X. Zhao, I.P. Georgakaki, M.L. Miller, R. Mejia-Rodriguez, C.-Y. Chiang, M.Y. Darensbourg, Inorg. Chem. 41 (2002) 3917;
(c) X. Zhao, C.-Y. Chiang, M.L. Miller, M.V. Rampersad, M.Y. Darensbourg, J. Am. Chem. Soc. 125 (2003) 518;
(d) I.P. Georgakaki, M.L. Miller, M.Y. Darensbourg, Inorg. Chem. 42 (2003) 2489;
(e) D. Chong, I.P. Georgakaki, R. Mejia-Rodriguez, J. Sanabria-Chinchilla, M.P. Soriaga, M.Y. Darensbourg, Dalton Trans. (2003) 4158.
[61] (a) A. Le Cloirec, S.P. Best, S. Borg, S.C. Davies, D.J. Evans, D.L. Hughes, C.J. Pickett, Chem. Commun. (1999) 2285;
(b) M. Razavet, A. Le Cloirec, S.C. Davies, D.L. Hughes, C.J. Pickett, J. Chem. Soc., Dalton Trans. (2001) 3551;
(c) M. Razavet, S.C. Davies, D.L. Hughes, C.J. Pickett, Chem. Commun. (2001) 847;
(d) M. Razavet, S.J. Borg, S.J. Georges, S.P. Best, S.A. Fairhurst, C.J. Pickett, Chem. Commun. (2002) 700;
(e) S.J. Georges, Z. Cui, M. Razavet, C.J. Pickett, Chem. Eur. J. 8 (2002) 4037;
(f) X. Yang, M. Razavet, X.-B. Wang, C.J. Pickett, L.-S. Wang, J. Phys. Chem. A 107 (2003) 4612;
(g) D.J. Evans, C.J. Pickett, Chem. Soc. Rev. 32 (2003) 268;
(h) S.J. Borg, T. Behrsing, S.P. Best, M. Razavet, X. Liu, C.J. Pickett, J. Am. Chem. Soc. 126 (2004) 16988.
[62] D. Sellmann, F. Geipel, M. Moll, Angew. Chem. Int. Ed. 39 (2000) 561;
D. Sellmann, R. Prakash, F.W. Heinemann, Eur. J. Inorg. Chem. (2004) 1847.
[63] (a) D. Sellmann, G.H. Rackelmann, F.W. Heinemann, Chem. Eur. J. 3 (1997) 2071;
(b) D. Sellmann, R. Prakash, F.W. Heinemann, Dalton Trans. (2004) 3991.
[64] D. Sellmann, F. Geipel, F. Lauderbach, F.W. Heinemann, Angew. Chem. Int. Ed. 114 (2002) 654;
D. Sellmann, F. Geipel, F.W. Heinemann, Chem. Eur. J. 8 (2002) 958.
[65] F.G. Bănică, Bull. Soc. Chim. Fr. 128 (1991) 697.
[66] S.-Q. Niu, M.B. Hall, Chem. Rev. 100 (2000) 353.
[67] R. Custelcean, J.E. Jackson, Chem. Rev. 101 (2001) 1963;
G.S. McGrady, G. Guilera, Chem. Soc. Rev. 32 (2003) 383.
[68] H.-J. Fan, M.B. Hall, J. Am. Chem. Soc. 123 (2001) 3828.
[69] S. Niu, M.B. Hall, Inorg. Chem. 40 (2001) 6201;
P.E.M. Siegbahn, M.R.A. Blomberg, M. Wirstam née Pavlov, R.H. Crabtree, J. Biol. Inorg. Chem. 6 (2001) 460, and references therein.
[70] M. Zimmer, G. Schulte, X.-L. Luo, R.H. Crabtree, Angew. Chem. Int. Ed. Engl. 30 (1991) 193.
[71] (a) J.C. Lee, A.L. Rheingold, B. Muller, P.S. Pregosin, R.H. Crabtree, J. Chem. Soc., Chem. Commun. (1994) 1021;
R.H. Crabtree, P.E.M. Siegbahn, O. Eisenstein, A.L. Rheingold, Acc. Chem. Res. 29 (1996) 348;
(b) D.-H. Lee, B.P. Patel, E. Clot, O. Eisenstein, R.H. Crabtree, Chem. Commun. (1999) 297;
(c) E. Peris, J.C. Lee Jr., J.R. Rambo, O. Eisenstein, R.H. Crabtree, J. Am. Chem. Soc. 117 (1995) 3485;

(d) A.J. Lough, S. Park, R. Ramachandran, R.H. Morris, J. Am. Chem. Soc. 116 (1994) 8356;
(e) R.H. Morris, Can. J. Chem. 74 (1996) 1907.
[72] Y. Ohki, N. Matsuura, T. Marumoto, H. Kawaguchi, K. Tatsumi, J. Am. Chem. Soc. 125 (2003) 7978.
[73] H.S. Chu, C.P. Lau, K.Y. Wong, Organometallics 17 (1998) 2768.
[74] A. Cabalerro, F.A. Jalón, B.R. Manzano, Chem. Commun. (1998) 1879.
[75] Y. blum, D. Czarkie, Y. Rahamim, Y. Shvo, Organometallics 4 (1985) 1459;
C.P. Casey, S.W. Singer, D.R. Powell, R.K. Hayashi, M. Kavana, J. Am. Chem. Soc. 123 (2001) 1090;
A.H. Ell, J.B. Jognson, J.-E. Bäckvall, Chem. Commun. (2003) 1652.
[76] C.P. Casey, T.E. Vos, S.W. Singer, I.A. Guzei, Organometallics 21 (2002) 5038;
C.P. Casey, T.E. Vos, G.A. Bikzhanova, Organometallics 22 (2003) 901;
M.-J. Kim, Y.I. Chung, Y.K. Choi, H.K. Lee, D. Kim, J. Park, J. Am. Chem. Soc. 125 (2003) 11494.
[77] T. Ohkuma, R. Noyori, Angew. Chem. Int. Ed. 40 (2001) 40, and references therein.
[78] J.A. Ayllon, S.F. Sayers, S. Sabo-Etienne, B. Donnadieu, B. Chaudret, Organometallics 18 (1999) 3981.
[79] S. Ott, M. Kritikos, B. Ackermark, L. Sun, R. Lomoth, Angew. Chem. Int. Ed. 43 (2004) 1006.
[80] P.G. Jessop, R.H. Morris, Inorg. Chem. 32 (1993) 2236.
[81] D. Sellmann, R. Prakash, F.W. Heinemann, M. Moll, M. Klimowicz, Angew. Chem. Int. Ed. 43 (2004) 1877.
[82] (a) Z.K. Sweeney, J.L. Polse, R.A. Andersen, R.G. Bergman, M.G. Kubinec, J. Am. Chem. Soc. 119 (1997) 4543;
Z.K. Sweeney, J.L. Polse, R.G. Bergman, R.A. Andersen, Organometallics 18 (1999) 5502;
(b) C. Bianchini, C. Mealli, A. Meli, M. Sabat, Inorg. Chem. 25 (1986) 4617;
(c) R.C. Linck, R.J. Pafford, T.B. Rauchfuss, J. Am. Chem. Soc. 123 (2001) 8856;
(d) H. Kato, H. Seino, Y. Misobe, M. Hidai, J. Chem. Soc., Dalton Trans. (2002) 1494;
(e) M.G. Basallote, M. Feliz, M.J. Fernandez-Trujillo, R. Llusar, V.S. Safont, S. Uriel, Chem. Eur. J. 10 (2004) 1463;
(f) C. Bianchini, A. Meli, Inorg. Chem. 26 (1987) 4268;
C. Bianchini, C. Mealli, A. Meli, M. Sabat, Inorg. Chem. 25 (1986) 4618.
[83] R. Bau, R.G. Teller, S.W. Kirtley, T.F. Kötzle, Acc. Chem. Res. 12 (1979) 176.
[84] S. Ogo, H. Nakai, Y. Watanabe, J. Am. Chem. Soc. 124 (2002) 597.
[85] G. Meister, G. Rheinwald, H. Stœckli-Evans, G. Süss-Fink, J. Chem. Soc., Dalton Trans. (1994) 325;
M. Jahncke, G. Meister, G. Rheinwald, H. Stœckli-Evans, G. Süss-Fink, Organometallics 16 (1997) 1137.
[86] P.G. Jessop, R.H. Morris, Coord. Chem. Rev. 121 (1992) 155.
[87] R.G. Pearson, Chem. Rev. 85 (1985) 41.
[88] R.H. Morris, Inorg. Chem. 31 (1992) 1471.
[89] A.B.P. Lever, Inorg. Chem. 29 (1990) 1271.
[90] G. Jia, A.J. Lough, R.H. Morris, Organometallics 11 (1992) 161.
[91] R. Ciancanelli, B.C. Noll, D.L. DuBois, M.R. DuBois, J. Am. Chem. Soc. 124 (2002) 2984.
[92] J.W. Raebiger, A. Miedaner, C.J. Curtis, S.M. Miller, O.P. Anderson, D.L. DuBois, J. Am. Chem. Soc. 126 (2004) 5502.
[93] P.J. Toscano, T.F. Swider, L.G. Marzilli, N. Breciani-Pahor, L. Randaccio, Inorg. Chem. 22 (1983) 3416.